PLOS ONE

RESEARCH ARTICLE

Piperidine scaffold as the novel P2-ligands in cyclopropyl-containing HIV-1 protease inhibitors: Structure-based design, synthesis, biological evaluation and docking study

Huiyu Zhou[1], Mei Zhu[1], Ling Ma[1], Jinming Zhou[2], Biao Dong[1], Guoning Zhang[1], Shan Cen[1], Yucheng Wang[1]*, Juxian Wang[1]*

1 Institute of Medicinal Biotechnology, Chinese Academy of Medical Science and Peking Union Medical College, Beijing, China, **2** Key Laboratory of the Ministry of Education for Advanced Catalysis Materials, Department of Chemistry, Zhejiang Normal University, Jinhua, China

* wyc9999@126.com (YW); imbjxwang@163.com (JW)

Citation: Zhou H, Zhu M, Ma L, Zhou J, Dong B, Zhang G, et al. (2020) Piperidine scaffold as the novel P2-ligands in cyclopropyl-containing HIV-1 protease inhibitors: Structure-based design, synthesis, biological evaluation and docking study. PLoS ONE 15(7): e0235483. https://doi.org/10.1371/journal.pone.0235483

Editor: A Ganesan, University of East Anglia, UNITED KINGDOM

Received: April 10, 2020

Accepted: June 17, 2020

Published: July 22, 2020

Data Availability Statement: All relevant data are within the paper and its Supporting Information files.

Funding: This work is supported by National Science & Technology Major Project "Key New Drug Creation and Manufacturing Program", China (2019ZX09201001-003) and CAMS Innovation Fund for Medical Sciences (CIFMS 2016-I2M-1-011) to HZ. The funders had no role in study

Abstract

A series of potent HIV-1 protease inhibitors, containing diverse piperidine analogues as the P2-ligands, 4-substituted phenylsulfonamides as the P2'-ligands and a hydrophobic cyclopropyl group as the P1'-ligand, were designed, synthesized and evaluated in this work. Among these twenty-four target compounds, many of them exhibited excellent activity against HIV-1 protease with half maximal inhibitory concentration (IC_{50}) values below 20 nM. Particularly, compound **22a** containing a (*R*)-piperidine-3-carboxamide as the P2-ligand and a 4-methoxylphenylsulfonamide as the P2'-ligand exhibited the most effective inhibitory activity with an IC_{50} value of 3.61 nM. More importantly, **22a** exhibited activity with inhibition of 42% and 26% against wild-type and Darunavir (DRV)-resistant HIV-1 variants, respectively. Additionally, the molecular docking of **22a** with HIV-1 protease provided insight into the ligand-binding properties, which was of great value for further study.

Introduction

HIV-1 infection has become a serious threat to human beings around the world since the first case was reported in 1981 in the USA [1]. An estimated 37.9 million people lived with HIV-1 and 770 thousand people died from AIDS-related diseases in 2018, according to the Joint United Nations Programme on HIV/AIDS (UNAIDS)'s 2019 fact sheet on global HIV & AIDS statistics [2]. Fortunately, the emergence of a large variety of antiviral drugs, especially the application of HIV-1 protease inhibitors (PIs) in highly active antiretroviral therapy (HAART), made significant contributions to transforming HIV-1 infection from an inevitably fatal disease into a manageable chronic ailment [3, 4]. HIV-1 PIs serve as a critical therapeutic approach for the treatment of HIV-1 infection due to their ability to block the production of viral proteins for mature virions [4–6]. So the design of potent PIs continues to be essential for long-term control of HIV-1 infection and AIDS [7–10].

In an effort to develop structurally novel PIs that exhibit potent inhibitory activity, one of the major design strategies is to optimize ligand-binding site interactions with the active site

design, data collection and analysis, decision to publish, or preparation of the manuscript.

Competing interests: The authors have declared that no competing interests exist.

of HIV-1 protease (PR) [6, 11–15]. Recently, we reported a series of PIs incorporating a cyclopropyl as the P1'-ligand and morpholine derivatives as the P2-ligands [16]. Among which, compounds **A** and **B** in Fig 1 showed IC_{50} values of 53 nM and 47 nM, respectively. The molecular docking of compound **A** revealed that the small hydrophobic cyclopropyl group filled in the pocket of the S1 Appendix-subsite subtly [17–19]. However, the oxygen atom of morpholine in the P2-ligand formed weak van der Waals interaction with the backbone atoms, while the wrapped nitrogen atom failed to make contact with the active site, which might be amenable for the suboptimal activity. In view of the above phenomena, piperidine—a flexible heterocycle containing exposed nitrogen atom—was introduced as the P2-ligand in the newly designed HIV-1 PIs, with the aim of promoting extensive hydrogen bonding interactions or favorable van der Waals interactions with the backbone atoms in the corresponding S2 Appendix-subsite of PR. In addition, the effect of P2'-ligands incorporating functionalized 4-substituted phenylsulfonamides on HIV-1 protease inhibitory activity was investigated (Fig 2).

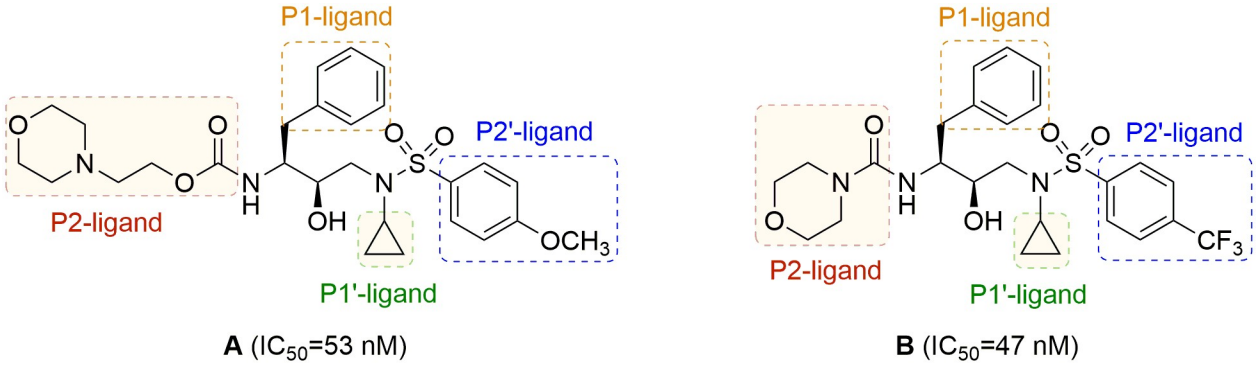

Fig 1. Structures of HIV-1 PIs A and B.

https://doi.org/10.1371/journal.pone.0235483.g001

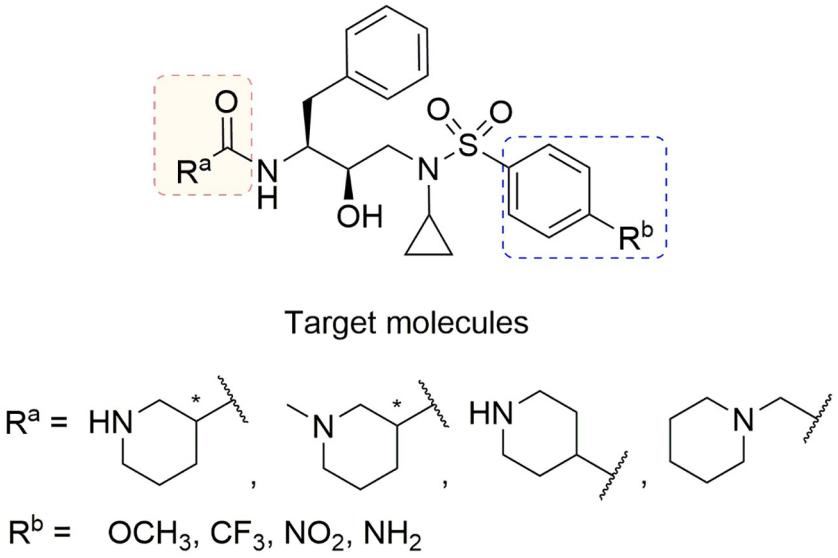

Fig 2. Chemical structures of target molecules.

https://doi.org/10.1371/journal.pone.0235483.g002

Materials and methods

Chemistry

The syntheses of substituted piperidine carboxylic acids **9–14** are shown in Scheme 1. All starting materials are commercially available. Chiral piperidine-3-carboxylic acids **1**, **2** and piperidine-4-carboxylic acid **3** were reacted with $(Boc)_2O$ in the presence of $NaHCO_3$ to obtain Boc-protected amine derivatives **9–11** in excellent yields (92.5–97.3%) [20]. Reaction of the optically active ethyl piperidine-3-carboxylates **4**, **5** with formaldehyde and formic acid in methanol at reflux for 6 h afforded the corresponding derivatives **7**, **8** in yields of 95.6% and 93.4%, respectively [21]. Saponification of **7** or **8** with aqueous sodium hydroxide provided corresponding carboxylic acids **12** or **13** in nearly quantitative yield. Treatment of piperidine **6** with bromoacetic acid and potassium carbonate in anhydrous DMF furnished **14** in 83.0% yield [11].

Scheme 1. Syntheses of substituted piperidine carboxylic acids 9–14. Reagents and conditions: (a) $(Boc)_2O$, $NaHCO_3$, THF/H_2O (1:1), Argon, 25 ˚C, overnight; (b) 40% formaldehyde, formic acid, MeOH, 0 ˚C to reflux, 6 h; (c) (i) NaOH, H_2O, 25 ˚C, 1 h; (ii) 1 N HCl, 0 ˚C, 0.5 h; (d) bromoacetic acid, K_2CO_3, anhydrous DMF, Argon, 25 ˚C, overnight.

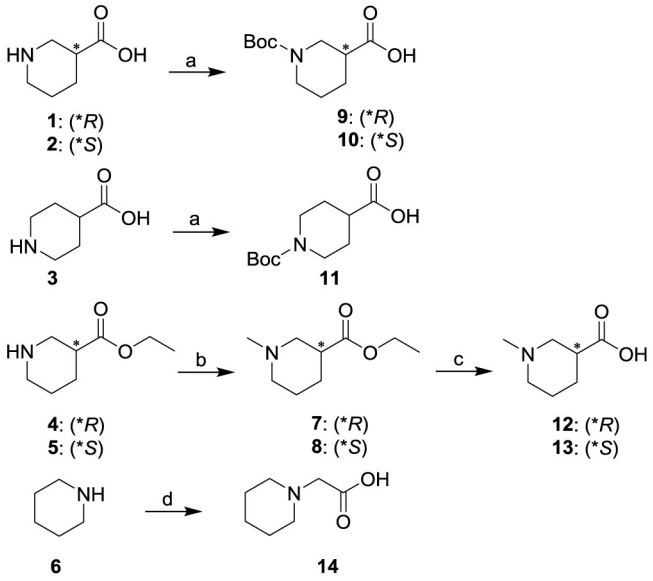

As depicted in Scheme 2, hydroxyethylamine sulfonamide isosteres **18a-d** were synthesized similarly according to the literature procedure [11, 16, 22]. Exposure of the commercially available epoxide **15** to cyclopropanamine in acetonitrile afforded amino alcohol **16** in 87.5% yield. Treatment of the resulting amino alcohol with 4-substituded-penzenesulfonly chlorides provided compounds **17a-c** in yields of 88.7–92.1%. They were subsequently converted to sulfonamide derivatives **18a-c** by deprotection of the Boc-group with trifluoroacetic acid in moderate yields (74.2–80.4%). Catalytic hydrogenation of **18c** over 10% Pd/C in a mixtre of ethyl acetate and methanol (1:2) for 4 h furnished aminosulfonamide derivate **18d** in 96.9% yield.

Scheme 2. Syntheses of hydroxyethylamine sulfonamide isosteres 18a-d. Reagents and conditions: (a) cyclopropanamine, acetonitrile, reflux, 7 h; (b) aryl sulfonyl chloride, DIEA, DMAP (Cat.), THF, 0–25 ˚C, overnight; (c) CF_3COOH/CH_2Cl_2 (1:3), 25 ˚C, 5 h; (d) H_2 (gas),

50 psi, 10% Pd/C, ethyl acetate/methanol (1:2), 25 ˚C, 4 h.

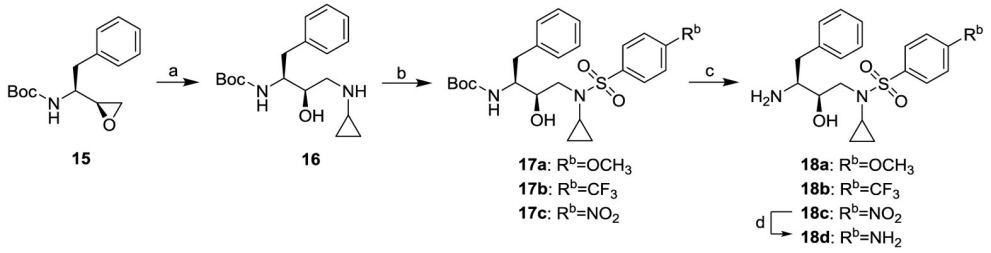

The syntheses of the target molecules **22a-27d** were illustrated in Scheme 3. Coupling of amines **18a-d** with acids **9–14** in the presence of EDCI, HOBt and catalytic amounts of DMAP obtained compounds **19a-21d**, **24a-25d** and **27a-d** in yields of 34.7–92.4%. Removal of the Boc-group by exposure of **19a-21d** to hydrogen chloride gas in CH_2Cl_2 provided corresponding piperidine derivatives **22a-23d** and **26a-d** in yields of 60.7–92.0%.

Scheme 3. Syntheses of inhibitors 22a-27d. Reagents and conditions: (a) EDCI, HOBt, DMAP, anhydrous DMF, Argon, 0–25 ˚C, 8 h; (b) HCl (gas), CH_2Cl_2, 25 ˚C, 0.5 h.

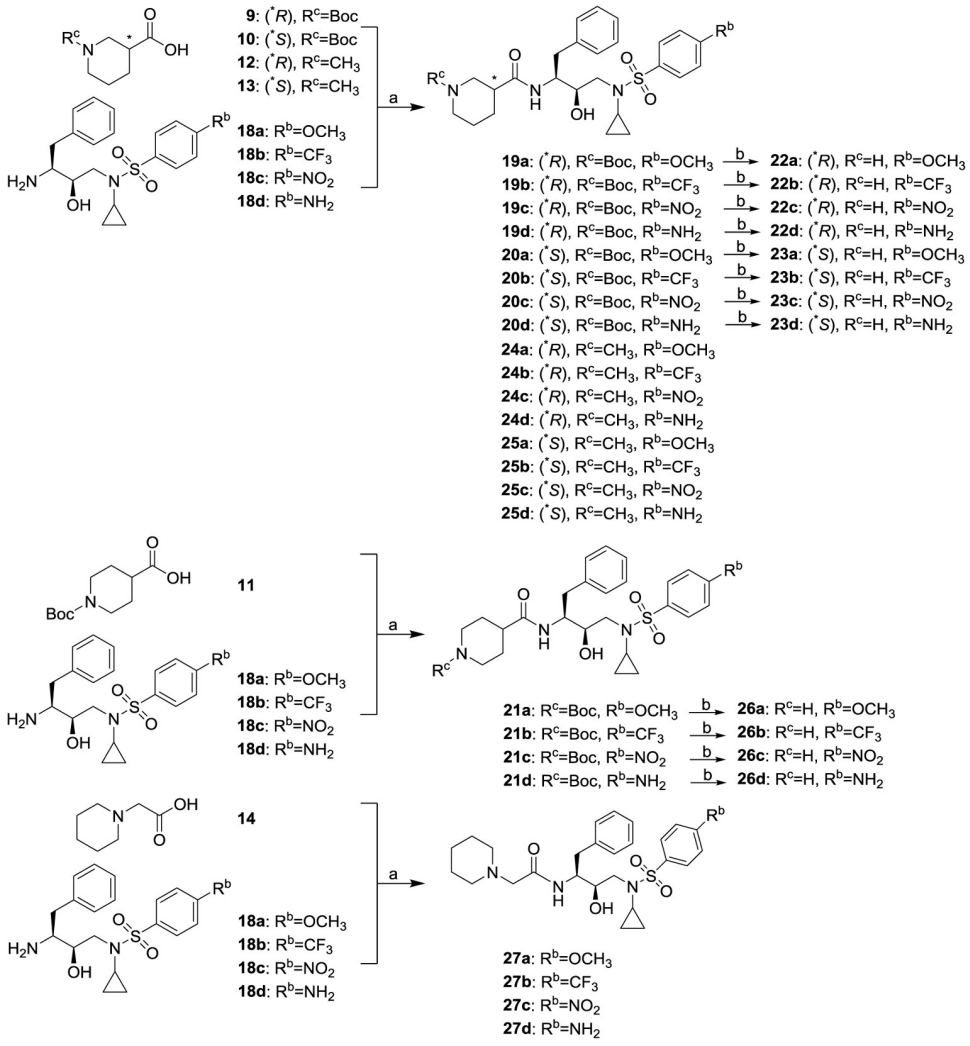

In vitro HIV-1 PR activity assay

The inhibitory effect of all new designed inhibitors were measured using fluorescence resonance energy transfer (FRET) method. Peptide (Arg-Glu (EDANS)-Ser-Gln-Asn-Tyr-Pro-Ile-Val-Gln- Lys(DABCYL)-Arg) purchased from AnaSpec was selected as the substrate. The energy transfer donor (EDANS) and acceptor (DABCYL) dyes are labeled at two ends of the peptide to perform FRET. Excitation and emission wavelengths were set at 340 nm and 490 nm. Inhibitors were dissolved in dimethylsulfoxide (DMSO) and diluted to appropriate concentrations. HIV-1 protease was cloned and heterologously expressed in Escherichia coli and purified. The experiment was carried out in 96-well plates. The FRET assay reaction buffer contained 0.1 M sodium acetate, 1 M sodium chloride, 1 mM ethylenediaminetetraacetic acid (EDTA), 1 mM dithiothreitol (DTT), 2% DMSO and 1 mg/mL bovine serum albumin (BSA) with an adjusted pH 4.7. Protease and inhibitor were mixed and incubated for 20–30 mins at room temperature and then the substrate was added. Each reaction was recorded for about 10 mins. From plots of concentration versus the calculated percent inhibition, IC_{50} values were determined.

HIV-1 infectivity assay

The inhibitory effect of compounds on HIV-1 infectivity were determined using a single-round HIV-1 infectivity assay. 293T cells were co-transfected with either plasmid pNL4-3-E$^-$R$^-$ (pHIV-1_{NL4-3}) or DRV-resistant pNL4-3-E$^-$R$^-$ variants (pHIV-$1_{DRV^R_S}$) and pHCMV-G (VSV-G) to produce VSV-G pseudotyped HIV-1. Inhibitors dissolved in dimethylsulfoxide (DMSO) and diluted to appropriate concentrations, were added into culture medium at 5 hours of post-transfection. After incubating for 48 hours at temperature 37 ˚C, pseudotyped viruses in 10 μL of supernatant were used to infect SupT1 cells for 48 hours, followed by measuring luciferase activity of newly infected cells using Centro LB960 (Berthold).

For the assay using wild type HIV-1, 1×10^6 SupT1 cells were infected with 100 μL HIV-1 NL4-3 in the presence of 100 nM chemicals and 10 μg/mL polybrene, keeping a total volume of 500 μL (Spin infection at 1800rpm, 45min). Cells were washed once in the next morning and medium were replaced with fresh medium containing 100 nM chemicals. At 48 hpi, viruses were harvested and 50 μL of viruses were used to infect TZM-bl cells, followed by measuring luciferase activity in the infected cells.

Cytotoxicity assay

Selected inhibitors were further evaluated in cytotoxicity assay using a cell counting kit-8 assay. Plates were prepared with 20 000 293T cells per well. After 24h of culture, 1μL of drugs were added to each well. After another 24h of culture, 10 μL of CCK-8 was added to each well. Absorbance was quantified at wavelength 450 nm using an EnVision multilabel reader (PerkinElmer) after 2h at room temperature. The 50% cytotoxic concentrations (CC_{50}) were determined as the concentration required to reduce the number of the cells by 50% compared to that of drug-unexposed control cultures.

Molecular docking

In general, the docking was performed through "DOCK" module in the Molecular Operating Environment (MOE) using the alpha triangle placement method. Refinement of the docked poses was carried out using the Forcefield refinement scheme and scored using both the affinity dG and london dG scoring system. The pose with the higher docking negative score implied better binding.

Results and discussion

Structure activity relationships

All target compounds were evaluated the inhibitory potency against wild-type HIV-1 PR using the fluorescence resonance energy transfer (FRET) method, including DRV as the positive control [23, 24]. The results are presented in Figs 3–5. As can be seen, the piperidine-derived inhibitors exhibited potent enzymatic activity with IC_{50} values of submicromolar to nanomolar

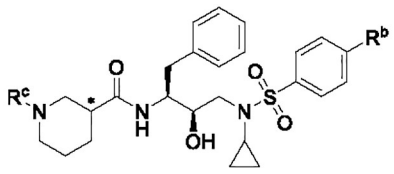

Compd.	R^c	*R/S	R^b	IC_{50} (nM)[1]	CC_{50} (μM)[1]	Compd.	R^c	*R/S	R^b	IC_{50} (nM)[1]	CC_{50} (μM)[1]
22a	H	*R*	OCH_3	3.61±1.59	> 100	**24a**	CH_3	*R*	OCH_3	8.07±3.59	> 100
22b	H	*R*	CF_3	8.35±5.58	> 100	**24b**	CH_3	*R*	CF_3	9.28±5.66	> 100
22c	H	*R*	NO_2	17.0±8.12	> 100	**24c**	CH_3	*R*	NO_2	39.5±11.9	-[2]
22d	H	*R*	NH_2	10.1±6.71	> 100	**24d**	CH_3	*R*	NH_2	16.3±9.54	> 100
23a	H	*S*	OCH_3	433±97.5	-	**25a**	CH_3	*S*	OCH_3	283±36.4	-
23b	H	*S*	CF_3	264±69.1	-	**25b**	CH_3	*S*	CF_3	110±27.2	-
23c	H	*S*	NO_2	483±103	-	**25c**	CH_3	*S*	NO_2	523±104	-
23d	H	*S*	NH_2	313±58.1	-	**25d**	CH_3	*S*	NH_2	236±36.5	-
DRV	-	-	-	0.82±0.17	> 100						

[1] All assays were conducted in triplicate, and the data shown represent mean values (±1 standard deviation) derived from the results of three independent experiments.

[2] The cytotoxicity of compounds with IC_{50} values higher than 20 nM was not assayed.

Fig 3. Enzymatic inhibitory activity and cytotoxicity of inhibitors 22a-25d.

https://doi.org/10.1371/journal.pone.0235483.g003

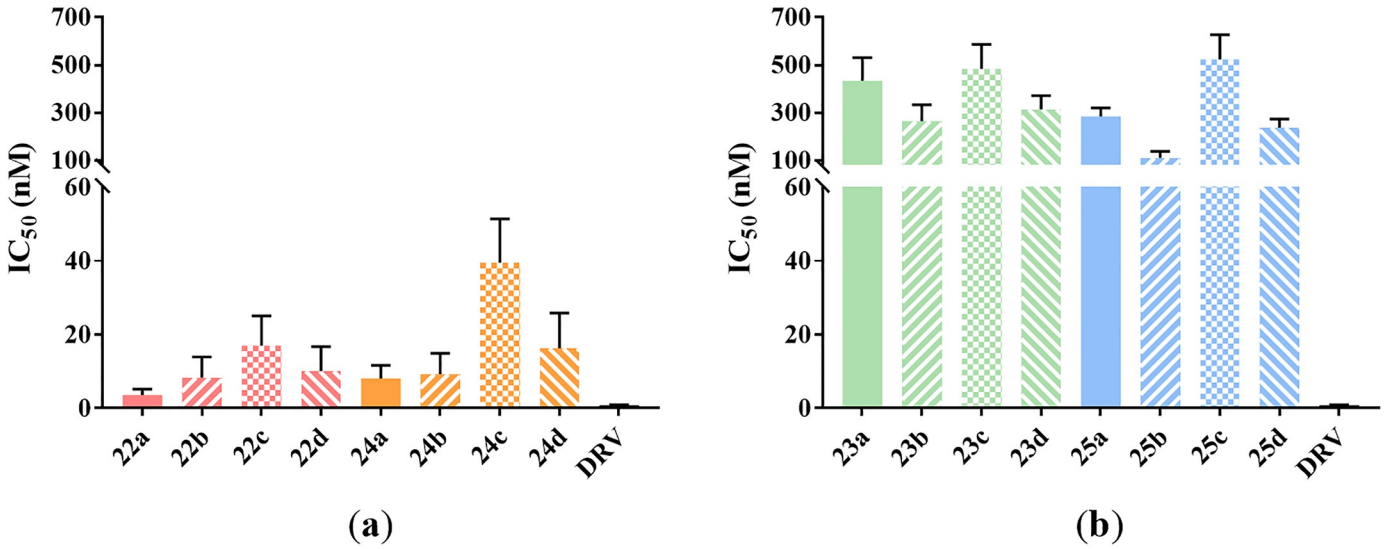

Fig 4. Enzymatic inhibitory activity of inhibitors. (a) Enzymatic inhibitory activity of inhibitors with (*R*)-piperidine derivatives as the P2-ligands; (b) Enzymatic inhibitory activity of inhibitors with (*S*)-piperidine derivatives as the P2-ligands.

https://doi.org/10.1371/journal.pone.0235483.g004

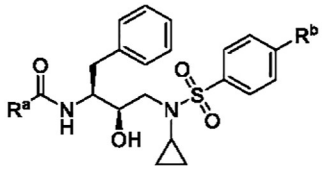

Compd.	R^a	R^b	IC_{50} (nM)[1]	Compd.	R^a	R^b	IC_{50} (nM)[1]
26a	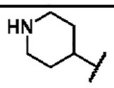	OCH_3	155±15.1	**27a**	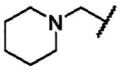	OCH_3	228±45.0
26b	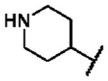	CF_3	124±27.6	**27b**	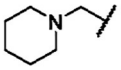	CF_3	52.7±14.7
26c	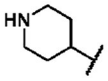	NO_2	268±37.8	**27c**	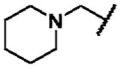	NO_2	288±62.0
26d	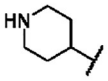	NH_2	245±39.8	**27d**	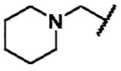	NH_2	34.7±12.5
DRV	-	-	0.82±0.17				

[1] All assays were conducted in triplicate, and the data shown represent mean values (±1 standard deviation) derived from the results of three independent experiments.

Fig 5. Enzymatic inhibitory activity of inhibitors 26a-27d.

https://doi.org/10.1371/journal.pone.0235483.g005

in general. Especially, inhibitor **22a**, containing a (*R*)-piperidine-3-carboxamide as the P2-ligand and a 4-methoxylphenylsulfonamide as the P2'-ligand, displayed the most impressive activity with an IC_{50} value of 3.61 nM.

As it turned out in Figs 3 and 4, inhibitors with (*R*)-piperidine derivatives as the P2-ligands exhibited superior activity than those with (*S*)-configuration as a whole. For instance, compound **22a** showed a 120-fold improvement of potency over **23a**, which revealed the significance of configurations. In addition, the activity decreased when the nitrogen atom of (*R*)-piperidine scaffold was methylated, such as **22a** *vs* **24a**, **22b** *vs* **24b**, **22c** *vs* **24c**, and **22d** *vs* **24d**. The results might be attributed to both the smaller volume of the P2-ligand which was more suitable for the cavity of S2 Appendix-subsite and the capacity of the exposed nitrogen atom which could form hydrogen bonding interactions with the carbonyl oxygen or amide NHs of Asp30 and Asp29 [25–28].

The functional P2'-ligands also exerted great impact on the potency of inhibitors. Compounds containing 4-methoxyl (**22-25a**), 4-trifluoromethyl (**22-25b**) and 4-amino (**22-25d**) substituents exhibited more potent enzyme inhibitory than the corresponding 4-nitro substituent compounds (**22-25c**). The oxygen atom of methoxyl group is capable of forming hydrogen bonds with the backbone NH and side-chain carboxylate of Asp30' directly, which could enhance the antiviral potency [29]. The 4-trifluoromethyl group in the P2'-ligand may cause favorable halogen interactions and van der Waals interactions with the P2'-pocket [30, 31], in spite of its weak electron-withdrawing inductive effect that impaired the binding affinity slightly [15]. Although the amino of 4-aminobenzene sulfonamide could participate in direct or water-mediated hydrogen bonds with Asp30', these interactions were weaker than those between 4-methoxybenzene sulfonamide and the cavity of S2 Appendix-subsite [10]. On the contrary, the strong electron-withdrawing property of nitro in the P2'-ligand, including both electron-withdrawing inductive effect and conjugation, was likely to weaken not only the hydrogen bonds between the nitro oxygen and Asp30', but also the water-mediated interactions between the sulfonyl oxygen and Ile50' [19, 15].

Furthermore, the cytotoxicity of selected inhibitors was assayed [32]. Surprisingly, all of them exhibited low cytotoxicity. Therefore, this kind of inhibitors with potent activity and low toxicity deserved in-depth study.

However, compounds **26a** and **27a** bearing 4- or 1-subsituted piperdine derivatives in Fig 5 showed more than 50-fold loss of potency over the 3-subsituted piperidine derivative **22a**. The same trend can also be observed in the other three groups (**22** *vs* **26**, **27b**; **22** *vs* **26**, **27c**; **22** *vs* **26**, **27d**), which suggested that the shift of substituent position and the length of linker can impact the activity remarkably. Moreover, the effect of functional P2'-ligands on potency is similar to that shown in Fig 3.

HIV-1 infectivity assay

In the assays against HIV-1 wild-type and DRV-resistant variants [33, 34], selected compounds **22a**, **24a** and **24b** exhibited inhibition activity to some extent (Fig 6). Notably, **22a** exhibited the most remarkable activity with inhibition of 42% and 26% against wild-type and DRV-resistant HIV-1 variants, respectively, which agreed with the activity tested *in vitro*. Although compounds **24a** and **24b** showed inconspicuous inhibition (with 16% and 12% against wild-type variants, and 8% and 7% against DRV-resistant variants, respectively), there still revealed regularity. Generally, compounds with 4-methoxylphenylsulfonamide as the P2'-ligand exhibited superior activity than those with 4-trifluoromethylphenylsulfonamide as the P2'-ligand *in vivo*, which pointed the way for further study.

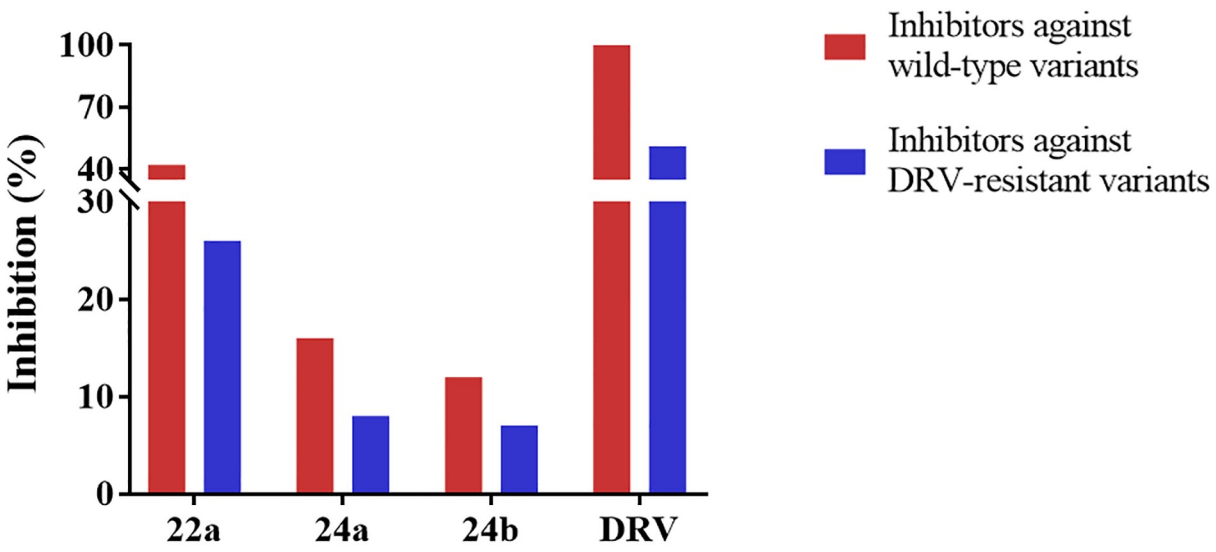

Fig 6. Inhibition of inhibitors against wild-type and DRV-resistant HIV-1 variants. Inhibition of inhibitors 22a, 24a and 24b was conducted at the concentration of 10 μM, and DRV at 20 nM.

https://doi.org/10.1371/journal.pone.0235483.g006

Molecular docking

In order to gain insight into the ligand-binding site interactions, the molecular modeling for **22a** was done in the molecular modeling software MOE with a HIV-1 PR crystal structure (PDB-ID: 4mc9) [35]. Remarkably, **22a** fitted into the active site of PR perfectly. As illustrated in Fig 7, several hydrogen bonding interactions were formed between the scaffold of the inhibitor and the residues Asp25, Ile50 (A chain) and Ile50 (B chain). Furthermore, plentiful van der Waals interactions between atoms in the P2-ligand, P1-ligand, P1'-ligand or P2'-ligand and external enzyme atoms were also observed. Especially, the newly introduced piperidine could produce favorable interactions with the active site of PR and be inserted into the cavity of S2 Appendix-subsite properly. All of the above mentioned might be responsible for the promising inhibitory activity of **22a**.

Conclusions

In summary, we have reported the structure-based design and synthesis of a series of novel HIV-1 PIs incorporating flexible piperidine moieties as the P2-ligands, 4-substituted phenylsulfonamides as the P2'-ligands and a cyclopropyl group as the P1'-ligand. Introduction of poperidine in the P2-ligand was for the sake of promoting hydrogen bonding or van der Waals interactions with the active site of HIV-1 PR backbone. A number of inhibitors exhibited excellent potency and low cytotoxicity. In particular, inhibitor **22a** containing a (*R*)-piperidine-3-carboxamide as the P2-ligand and a 4-methoxylphenylsulfonamide as the P2'-ligand showed the most remarkable enzyme inhibitory activity, with an IC_{50} value of 3.61 nM, as well as activity with inhibition of 42% and 26% against wild-type and DRV-resistant HIV-1 variants, respectively. We demonstrated that the stereochemistry and substitution position of piperidine derivatives in the P2-ligands, as well as functional phenylsulfonamides in the P2'-ligands, are decisive for the potency. Moreover, the molecular docking of **22a** showed that the piperidine could fill in the pocket of S2 Appendix-subsite perfectly and make strong interactions with residues of HIV-1 PR, which was consistent with its potent antiviral activity. Further

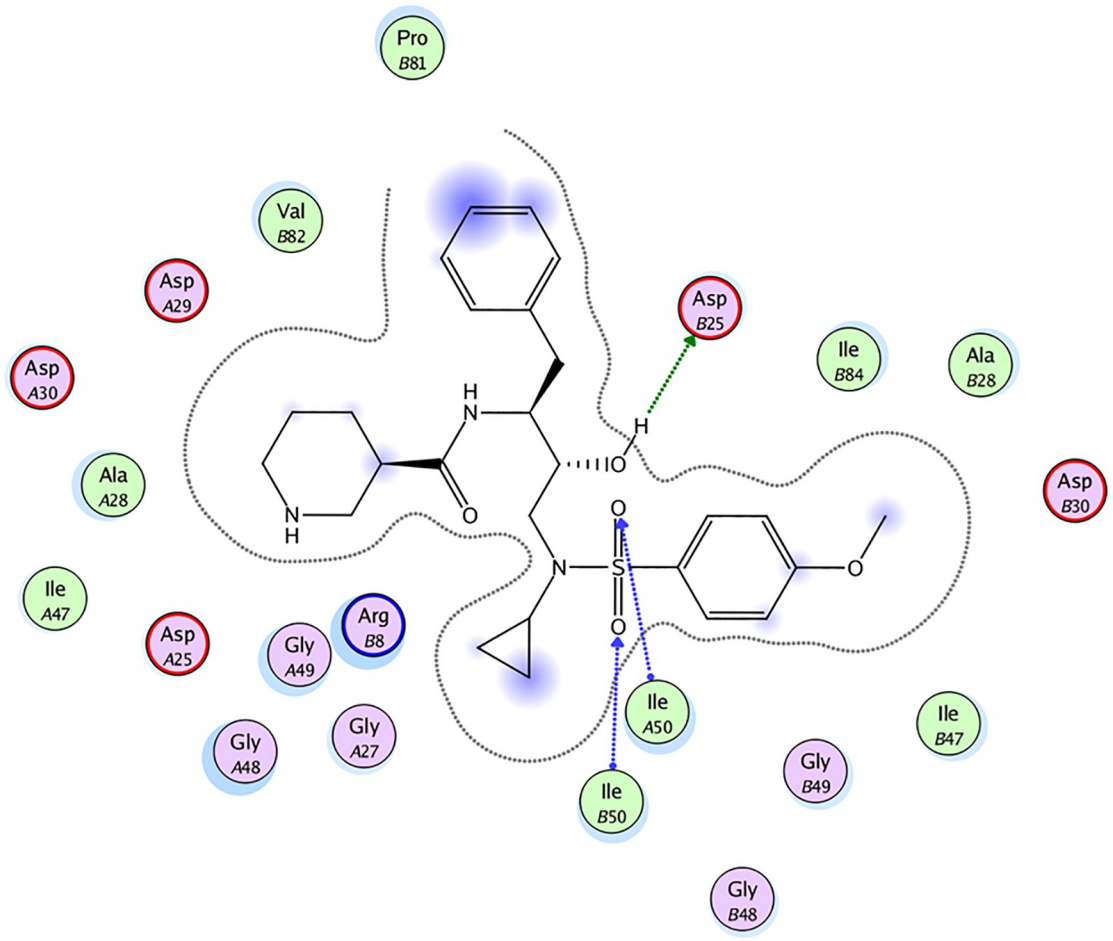

Fig 7. Docking of 22a in HIV-1 PR. Ligand exposures are described as purple spheres. Hydrogen bonding interactions between ligands and residues are represented as blue or green arrows.

https://doi.org/10.1371/journal.pone.0235483.g007

studies on the evaluation of other flexible *N*-containing heterocycle derivatives are currently in progress.

Supporting information

S1 Appendix. Description of synthetic experiments.
(DOCX)

S2 Appendix. ^{1}H NMR, ^{13}C NMR and HR MS spectrums of compounds.
(DOCX)

S3 Appendix. Description of biological evaluation and docking study.
(DOCX)

Acknowledgments

We would like to thank the Department of Virology for *in vitro* HIV-1 PR activity assay and cytotoxicity assay, Department of Immunology for HIV-1 infectivity assay and providing the Molecular Operating Environment for molecular docking.

Author Contributions

Data curation: Guoning Zhang.

Formal analysis: Ling Ma.

Investigation: Huiyu Zhou, Ling Ma, Jinming Zhou, Biao Dong, Shan Cen.

Methodology: Mei Zhu.

Resources: Shan Cen, Yucheng Wang.

Supervision: Juxian Wang.

Writing – original draft: Huiyu Zhou.

Writing – review & editing: Mei Zhu, Yucheng Wang, Juxian Wang.

References

1. Gottlieb MS, Schanker HM, Fan PT, Saxon A, Weisman JD, Pozalski. Pneumocystis pneumonia—Los Angeles. Morb Mortal Weekly Rep. 1981; 30(21): 1–3.
2. UNAIDS. Global HIV & AIDS statistics—2019 fact sheet. 2020; 3: 15. https://www.unaids.org/en/resources/fact-sheet
3. Mehellou Y, de Clercq E. Twenty-six years of anti-HIV drug discovery: where do we stand and where do we go? J Med Chem. 2010; 53(2): 521–538.
4. Ghosh AK, Osswald HL, Prato G. Recent Progress in the Development of HIV-1 Protease Inhibitors for the Treatment of HIV/AIDS. J Med Chem. 2016; 59(11): 5172–5208.
5. Bungard CJ, Williams PD, Schulz J, Wiscount CM, Holloway MK, Loughran HM, et al. Design and synthesis of piperazine sulfonamide cores leading to highly potent HIV-1 protease inhibitors. ACS Med Chem Lett. 2017; 8(12): 1292–1297.
6. Midde NM, Patters BJ, Rao PSS, Cory TJ, Kumar S. Investigational protease inhibitors as antiretroviral therapies. Expert Opin Investig Drugs. 2016; 25(10): 1189–1200.
7. Ghosh AK, Williams JN, Ho RY, Simpson HM, Hattori SI, Hayashi H, et al. Design and synthesis of potent HIV-1 protease inhibitors containing bicyclic oxazolidinone scaffold as the P2 ligands: Structure–activity studies and biological and X-ray structural studies. J Med Chem. 2018; 61(21): 9722–9737.
8. Ghosh AK, Williams JN, Kovela S, Takayama J, Simpson HM, Walters DE, et al. Potent HIV-1 protease inhibitors incorporating squaramide-derived P2 ligands: Design synthesis and biological evaluation. Bioorg Med Chem Lett. 2019; 29(18): 2565–2570.
9. Delino NS, Aoki M, Hayashi H, Hattori SI, Chang SB, Takamatsu Y, et al. GRL-079 a novel HIV-1 protease inhibitor is extremely potent against multidrug-resistant HIV-1 variants and has a high genetic barrier against the emergence of resistant variants. Antimicrob Agents Chemother. 2018; 62(5): e02060–17.
10. Rusere LN, Lockbaum GJ, Lee SK, Henes M, Kosovrasti K, Spielvogel E, et al. HIV-1 Protease Inhibitors Incorporating Stereochemically Defined P2′ Ligands To Optimize Hydrogen Bonding in the Substrate Envelope. J Med Chem. 2019; 62(17): 8062–8079.
11. Zhu M, Dong B, Zhang GN, Wang JX, Cen S, Wang YC. Synthesis and biological evaluation of new HIV-1 protease inhibitors with purine bases as P2-ligands. Bioorg Med Chem Lett. 2019; 29(12): 1541–1545.
12. Zhu M, Ma L, Zhou H, Dong B, Wang Y, Wang Z, et al. Preliminary SAR and biological evaluation of potent HIV-1 protease inhibitors with pyrimidine bases as novel P2 ligands to enhance activity against DRV-resistant HIV-1 variants. Eur J Med Chem. 2020; 185: 111866.
13. Zhu M, Ma L, Wen J, Dong B, Wang Y, Wang Z, et al. Rational design and Structure− Activity relationship of coumarin derivatives effective on HIV-1 protease and partially on HIV-1 reverse transcriptase. Eur J Med Chem. 2020; 186: 111900.
14. Yang ZH, Bai XG, Zhou L, Wang JX, Liu HT, Wang YC. Synthesis and biological evaluation of novel HIV-1 protease inhibitors using tertiary amine as P2-ligands. Bioorg Med Chem Lett. 2015; 25(9): 1880–1883.
15. Bai X, Yang Z, Zhu M, Dong B, Zhou L, Zhang G, et al. Design and synthesis of potent HIV-1 protease inhibitors with (S)-tetrahydrofuran-tertiary amine-acetamide as P2− ligand: Structure− activity studies and biological evaluation. Eur J Med Chem. 2017; 137: 30–44.

16. Dou Y, Zhu M, Dong B, Wang JX, Zhang GN, Zhang F, et al. Design synthesis and biological evaluation of HIV-1 protease inhibitors with morpholine derivatives as P2 ligands in combination with cyclopropyl as P1′ ligand. Bioorg Med Chem Lett. 2020; 30(7): 127019.
17. He M, Zhang H, Yao X, Eckart M, Zuo E, Yang M. Design Biologic Evaluation and SAR of Novel Pseudo-peptide Incorporating Benzheterocycles as HIV-1 Protease Inhibitors. Chem Biol Drug Des. 2010; 76(2): 174–180.
18. Amin SA, Adhikari N, Bhargava S, Jha T, Gayen S. Structural exploration of hydroxyethylamines as HIV-1 protease inhibitors: new features identified. SAR QSAR Environ Res. 2018; 29(5): 385–408.
19. Ghosh AK, Chapsal BD. Design of the anti-HIV protease inhibitor darunavir. In: Ganellin CR, Jefferis R, Roberts SM, editors. Introduction to biological and small molecule drug research and development: theory and case studies. Elsevier; 2013. pp. 355–384.
20. Bell JL, Haak AJ, Wade SM, Kirchhoff PD, Neubig RR, Larsen SD. Optimization of novel nipecotic bis (amide) inhibitors of the Rho/MKL1/SRF transcriptional pathway as potential anti-metastasis agents. Bioorg Med Chem Lett. 2013; 23(13): 3826–3832.
21. Biofocus PLC Ward T Crossley R. WO2004/58259 2004 A1.
22. Ghosh AK, Sridhar PR, Leshchenko S, Hussain AK, Li J, Kovalevsky AY, et al. Structure-based design of novel HIV-1 protease inhibitors to combat drug resistance. J Med Chem. 2006; 49(17): 5252–5261.
23. Matayoshi ED, Wang GT, Krafft GA, Erickson J. Novel fluorogenic substrates for assaying retroviral proteases by resonance energy transfer. Science. 1990; 247(4945): 954–958.
24. Gregson SJ, Howard PW, Hartley JA, Brooks NA, Adams LJ, Jenkins TC, et al. Design synthesis and evaluation of a novel pyrrolobenzodiazepine DNA-interactive agent with highly efficient cross-linking ability and potent cytotoxicity. J Med Chem. 2001; 44(5): 737–748.
25. Gao BL, Zhang CM, Yin YZ, Tang LQ, Liu ZP. Design and synthesis of potent HIV-1 protease inhibitors incorporating hydroxyprolinamides as novel P2 ligands. Bioorg Med Chem Lett. 2011; 21(12): 3730–3733.
26. Parai MK, Huggins DJ, Cao H, Nalam MN, Ali A, Schiffer CA, et al. Design synthesis and biological and structural evaluations of novel HIV-1 protease inhibitors to combat drug resistance. J Med Chem. 2012; 55(14): 6328–6341.
27. Kovalevsky AY, i F, Leshchenko S, Ghosh AK, Louis JM, Harrison RW, et al. Ultra-high resolution crystal structure of HIV-1 protease mutant reveals two binding sites for clinical inhibitor TMC114. J Mol Biol. 2006; 363(1): 161–173.
28. Ghosh AK, Yu X, Osswald HL, Agniswamy J, Wang YF, Amano M, et al. Structure-Based Design of Potent HIV-1 Protease Inhibitors with Modified P1-Biphenyl Ligands: Synthesis Biological Evaluation and Enzyme–Inhibitor X-ray Structural Studies. J Med Chem. 2015; 58(13): 5334–5343.
29. Ghosh AK, Leshchenko-Yashchuk S, Anderson DD, Baldridge A, Noetzel M, Miller H B, et al. Design of HIV-1 protease inhibitors with pyrrolidinones and oxazolidinones as novel P1′-ligands to enhance backbone-binding interactions with protease: Synthesis biological evaluation and protein− ligand x-ray studies. J Med Chem. 2009; 52(13): 3902–3914.
30. Aoki M, Hayashi H, Rao KV, Das D, Higashi-Kuwata N, Bulut H, et al. A novel central nervous system-penetrating protease inhibitor overcomes human immunodeficiency virus 1 resistance with unprecedented aM to pM potency. eLife. 2017; 6: e28020.
31. Ghosh AK, Rao KV, Nyalapatla PR, Kovela S, Brindisi M, Osswald HL, et al. Design of Highly Potent Dual-Acting and Central-Nervous-System-Penetrating HIV-1 Protease Inhibitors with Excellent Potency against Multidrug-Resistant HIV-1 Variants. ChemMedChem. 2018; 13(8): 803–815.
32. Tominaga H, Ishiyama M, Ohseto F, Sasamoto K, Hamamoto T, Suzuki K, et al. A water-soluble tetrazolium salt useful for colorimetric cell viability assay. Anal Commun. 1999; 36(2): 47–50.
33. Aoki M, Das D, Hayashi H, Aoki-Ogata H, Takamatsu Y, Ghosh AK, et al. Mechanism of Darunavir (DRV)'s High Genetic Barrier to HIV-1 Resistance: A Key V32I Substitution in Protease Rarely Occurs, but Once It Occurs, It Predisposes HIV-1 To Develop DRV Resistance. mBio. 2018; 9(2):e02425–17.
34. Garcia JM, Gao A, He PL, Choi J, Tang W, Bruzzone R, et al. High-throughput screening using pseudotyped lentiviral particles: a strategy for the identification of HIV-1 inhibitors in a cell-based assay. Antiviral Res. 2009; 81(3):239–247.
35. Ganguly AK, Alluri SS, Wang CH, Antropow A, White A, Caroccia D, et al. Structural optimization of cyclic sulfonamide based novel HIV-1 protease inhibitors to picomolar affinities guided by X-ray crystallographic analysis. Tetrahedron. 2014; 70(18): 2894–2904.